# $Bi^{3+}$-$Pr^{3+}$ energy transfer processes and luminescent properties of LuAG:Bi,Pr and YAG:Bi,Pr single crystalline films

**[1,2]Y. Zorenko[*], [2]V. Gorbenko, [2]V. Savchyn, [2]T. Zorenko, [3]M. Nikl, [3]J.A. Mares, [3]A. Beitlerova, [3]V. Jary**

*[1]Institute of Physics of Kazimierz Wielki University in Bydgoszcz, Powstańców Wielkopolskich str.,2, 85-090 Bydgoszcz, Poland*
*[2]Laboratory of Optoelectronic Materials (LOM), Department of Electronics of Ivan Franko National University of Lviv, Gen. Tarnavskyj str., 107, 70017 Lviv, Ukraine*
*[3]Institute of Physics of Academy of Sciences of Czech Republic*
*[4]Cukrovarnicka str., 10, 162 53 Prague, Czech Republic*

**Abstract**
Absorption, cathodoluminescence, excitation spectra of photoluminescence (PL) and PL decay kinetics were studied at 300 K for the double doped $Bi^{3+}$-$Pr^{3+}$ and separately doped $Bi^{3+}$ and $Pr^{3+}$ $Lu_3Al_5O_{12}$ (LuAG) and $Y_3Al_5O_{12}$ (YAG) single crystalline film (SCF) phosphors grown by the liquid phase epitaxy method. The emission bands in the UV range arising from the intrinsic radiative transitions of $Bi^{3+}$-based centers, and emission bands in the visible range, related to the luminescence of excitons localized around Bi-based centers, were identified in both Bi-Pr and Bi-doped LuAG and YAG SCFs. The energy transfer processes from the host lattice simultaneously to $Bi^{3+}$ and $Pr^{3+}$ ions and from $Bi^{3+}$ to $Pr^{3+}$ ions were investigated. Competition between $Pr^{3+}$ and $Bi^{3+}$ ions in the energy transfer processes from the LuAG and YAG hosts was evidenced. The strong decrease of the $Pr^{3+}$ luminescence intensity in both LuAG:Pr and YAG:Pr SCF phosphors, grown from $Bi_2O_3$ flux, is observed due to the quenching influence of $Bi^{3+}$ flux related impurity. Due to overlap of the UV emission band of $Bi^{3+}$ centers with the f-d absorption bands of $Pr^{3+}$ ions in the UV range and the luminescence of excitons localized around Bi ions with the f-f absorption bands of $Pr^{3+}$ ions in the visible range, an effective energy transfer from $Bi^{3+}$ ions to $Pr^{3+}$ ions takes place in LuAG:Bi,Pr and YAG:Bi,Pr SCFs, resulting in the appearance of slower component in the decay kinetics of the $Pr^{3+}$ d-f luminescence.

*Keywords*: luminescence; energy transfer; garnets; single crystalline films, $Bi^{3+}$ and $Pr^{3+}$ ions
*PACS*: 78.55.Hx; 78.47.+p; 71.55.-i

## 1. Introduction

The $Pr^{3+}$ doped $Lu_3Al_5O_{12}$ (LuAG) and $Y_3Al_5O_{12}$ (YAG) garnets possess an intense and fast emission in the ultraviolet (290-400 nm) range due to the 5d-4f radiative transitions of $Pr^{3+}$ ions and are being considered now as prospective scintillators and cathodoluminescence screens for different applications [1-8]. The Pr-doped YAG and LuAG–based scintillators can be prepared both in the form of bulk single crystals (SC) by the Czochralski or Bridgman methods [1-8] as well as in the form of single crystalline films (SCF) by the Liquid Phase Epitaxy (LPE) method with a typical thickness of 2-60 μm [9-12]. Apart from the traditional scintillation applications for environmental radiation monitoring and positron emission tomography (PET) [3, 4, 7, 8], they can be employed also for imaging screens with high spatial resolution [9, 13-16] with some advantages with respect to typical powder phosphor-based screens [17]. Specifically, due to location of the emission spectra of LuAG:Pr and YAG:Pr SCF in the UV range, the spatial resolution R of screens can be improved with respect to the Ce doped LuAG and YAG SCF based scintillating screens emitting in the visible range, according to the formula $R \sim 0.61 * \lambda/NA$ (1), where λ is the emission wavelength, NA is the numerical aperture of the optics [9, 10, 15, 16].

Under excitation in the range of band-to-band transitions of YAG and LuAG hosts, the intense complex slow intrinsic luminescence arises in the melt-grown undoped and $Pr^{3+}$ doped YAG and LuAG SCs in the UV spectral range [18-20]. This emission was related to the luminescence of exciton

* ***Corresponding author:*** zorenko@ukw.edu.pl

localized near the $Y_{Al}$ and $Lu_{Al}$ antisite defects (AD) and recombination emission of the $Y_{Al}$ and $Lu_{Al}$ ADs itself [19, 20]. The emission of AD-related centers partly is overlapped with the $Pr^{3+}$ absorption bands, which influence the timing characteristics of LuAG:Pr and YAG:Pr SC scintillators [6, 21, 22]. The $Y_{Al}$ and $Lu_{Al}$ ADs in YAG:Pr and LuAG:Pr SC can also play the role of shallow electron traps, which are responsible for intensive thermoluminescence peaks within 100-200 K [21, 22] and can be another reason for considerable amount of very slow decay components in the scintillation response of LuAG:Pr and YAG:Pr bulk SC scintillators [4, 18, 19].

In our previous works [18-20] we have found that the formation of $Y_{Al}$ and $Lu_{Al}$ ADs is completely suppressed in SCF grown by the LPE method. As a result of AD elimination, the YAG:Pr and LuAG:Pr SCFs, in principle, can possess better timing characteristics under excitation in the range of interband transitions with respect to their bulk SC analogues [20]. At the same time, at the preparation of SCF by LPE method usually from PbO-based fluxes, lead ions are also introduced into the garnet lattice [23] and can influence the luminescent and scintillation properties of rare-earth doped SCF phosphors [24]. Namely, the influence of Pb-related centers on the luminescence of $Pr^{3+}$ ions in LuAG and YAG SCF, grown from PbO-based flux, was investigated in detail in our previous works [11, 12].

Recently we have shown that the $Bi_2O_3$ flux also can be successfully applied for producing SCF scintillators based on garnets compounds, specifically LuAG:Bi and YAG:Bi SCFs [25, 26]. The absorption and luminescence of the Bi-containing centers in YAG and LuAG SCFs have been investigated by us in [25-29]. In particular, the absorption/excitation bands in the 265-280 nm and 200-210 nm ranges were ascribed to the $^1S_0 \rightarrow {}^3P_1$ and $^1S_0 \rightarrow {}^1P_1$ transition of $Bi^{3+}$ in YAG and LuAG hosts [25, 26, 30]. Excitation of YAG:Bi and LuAG:Bi SCF in the range of interband transitions results in the appearance of two Bi-related emission bands in the UV and visible (VIS) spectral ranges [25, 26, 31-33]. The luminescence in the UV and VIS bands is characterized by substantially different excitation spectra and emission decay what points to different nature and excitation mechanisms of Bi-related centers in the UV and VIS ranges [27-29]. Namely, the nature of the UV luminescence in YAG:Bi and LuAG:Bi we attribute to the intrinsic radiative $^3P_1 \rightarrow {}^1S_0$ transition of $Bi^{3+}$-based centers, when the emission bands in the VIS range we related to the luminescence of excitons localized around Bi-based centers [24-29]. At very large Bi concentration (above 0.15-0.2 at. %), the intensity of the UV band decreases but the intensity of the VIS band increases with increasing the concentration of Bi ions in the SCF due to formation of $Bi^{3+}$ dimer centers [25, 26]. The energy structure of single and dimer centers was also investigated by us in YAG:Bi and LuAG:Bi SCF under excitation by synchrotron radiation with an energy of 3.7-25 eV [29].

However, the influence of the Bi-related centers on the $Pr^{3+}$ luminescence characteristics in YAG and LuAG SCF phosphors has not been studied up to now. Therefore, the aim of this work is to study the phenomena related to the influence of the $Bi^{3+}$ ions on the luminescent properties of $Pr^{3+}$ doped YAG and LuAG-based SCF scintillators, namely: (i) to identify the spectral bands arising from the Bi-related centers in and LuAG:Pr and YAG:Pr SCF; (ii) to study the energy transfer processes from the YAG and LuAG hosts both to the $Bi^{3+}$ and $Pr^{3+}$ ions; (iii) to clarify the influence of $Bi^{3+}$-based centers on the luminescence characteristics of $Pr^{3+}$ ions in YAG:Pr and LuAG:Pr SCF phosphors.

## 2. SCF growth and experimental technique

The series of LuAG:Bi,Pr and YAG:Bi,Pr SCFs with dimensions of about 1×1 $cm^2$ and thicknesses between 12 and 60 μm were grown on (110) oriented YAG substrates at LOM, Lviv University, using the LPE method from super-cooled melt-solution based on $Bi_2O_3$ oxide flux. We did not use any co-doping to reduce a significant mismatch between the lattice constants of LuAG SCF (11.884 Å) and YAG substrate (11.999 Å). The concentration of $Pr_4O_7$ activating oxide with respect to the total content of garnet components in melt-solution was 1.5 mol % and 1.0 mol % in case of growth of LuAG:Pr,Bi and YAG:Pr,Bi SCFs, respectively. The concentration of crystal forming components with respect to the total content of melt-solution was 5.7-6.7 mol % and 5.6 mol %, respectively. These values determine the different temperatures of saturation of the respective melt-solutions $T_S$~1015 $^oC$ and ~1025 $^oC$ as well as the ranges of SCF growth temperatures $T_g$=945-980 $^oC$ and 955-975 $^oC$, respectively, see Table 1.

Table 1. Growth conditions and dopant content in (Y-Lu)AG:Bi,Pr, (Y-Lu)AG:Bi and (Y-Lu)AG:Pr SCFs grown prepared by LPE method from the $Bi_2O_3$ and PbO-based flux onto YAG substrates. $T_g$ – temperature of growth, h – SCF thickness;

| SCF sample | No of sample | Flux | $T_g$,°C | h, μm | Pb, at. % | Bi, at. % | Pr, at. % | LY, % |
|---|---|---|---|---|---|---|---|---|
| **YAG:Bi,Pr** | 8-14-3 | $Bi_2O_3$ | 970 | 9 | | 0.95 | 0.083 | ~11.5 |
| **LuAG:Bi,Pr** | 8-12-4 | $Bi_2O_3$ | 965 | 34 | | 1.59 | 0.43 | 13 |
| **YAG:Bi** | 8-10-3 | $Bi_2O_3$ | 968 | 21 | | 0.4 | - | 15.9 |
| **LuAG:Bi** | 7-8-4 | $Bi_2O_3$ | 953 | 12 | | 0.18 | - | 15.1 |
| **YAG:Pr** | 4 | PbO | 986 | 27 | > 0.01 | - | 0.225 | 37 |
| **LuAG:Pr** | 8 | PbO | 1005 | 43 | > 0.01 | - | 0.355 | 30 |
| **YAP:Ce SC** | | | | | | | | 100 |

The luminescent properties of the chosen two samples LuAG:Pr,Bi and YAG:Bi,Pr SCFs were compared with the properties of two respective samples of YAG:Bi and LuAG:Bi SCFs from our previous work [26] as well as with the properties of two samples YAG:Pr and LuAG:Pr SCF, grown from traditional $PbO-B_2O_3$ flux (see Table 1 and reference [11] for details).

The relative concentrations of $Bi^{3+}$ and $Pr^{3+}$ ions in all samples of the series of (Lu,Y)AG:Bi and (Lu,Y)AG:Bi,Pr SCFs were varied as function of the temperature of growth $T_g$, see Table 1. The dopant content of bismuth and praseodymium in Bi-, Pr- and Bi,Pr doped YAG and LuAG SCFs was determined using a JEOL JXA-733 electron microprobe analyzer and was found within 0.18-1.59 at. % and 0.083-0.355 at. % ranges, respectively, see Table 1. Due to the large ionic radius of $Bi^{3+}$ and $Pr^{3+}$ (1.17 and 1.126 Å for coordination 8 [34]), $Bi^{3+}$ and $Pr^{3+}$ ions are localized exclusively in the dodecahedral **{c}**–sites replacing $Y^{3+}$ or $Lu^{3+}$ cations in the garnet lattice.

The absorption spectra of Bi-, Pr- and Bi-Pr doped LuAG and YAG SCFs were measured using an UV/VIS/NIR absorption spectrophotometer Shimadzu UV-310 PC in the 190-800 nm wavelength range at 300 K.

The cathodoluminescent (CL) spectra of the SCF under study were recorded at 300 K with a set-up based on a DMR-4A monochromator and a PMT FEU-106 under pulsed e-beam excitation (duration of pulse of 2 μs and frequency of 30-3 Hz) with an energy of electrons of 9 keV and a beam current of 100 μA. The CL spectra were corrected for the sensitivity of detection part of the set-up.

The excitation spectra of $Pr^{3+}$ and $Bi^{3+}$ luminescence in the 3.7-25 eV range in LuAG:Pr, LuAG:Pr,Bi and YAG:Pr, YAG:Bi,Pr SCFs were investigated at 300 K at the Superlumi station at HASYLAB under excitation by synchrotron radiation (SR) with an energy of 3.7-25 eV. The excitation spectra were corrected for the spectral dependence of transmittance of Al-grating and intensity of SR beam.

The decay kinetics of the $Bi^{3+}$ and $Pr^{3+}$ luminescence at 300 K was measured with a modified Spectrofluorometer 199S (Edinburgh Instruments) under excitation with a nanosecond coaxial hydrogen-filled flash-lamp using single grating monochromators. The detection was performed with an TBX-04 photomultiplier module (IBH Scotland) using the method of time-correlated single photon counting. A deconvolution procedure (SpectraSolve software package) was applied to extract true decay times using the multi-exponential approximation.

The decay kinetics of the $Pr^{3+}$ luminescence was also measured at 300 K in the 0-200 ns time interval under excitation by synchrotron radiation with a pulse duration of 0.126 ns at the Superlumi station (HASYLAB, DESY).

The LY of the radioluminescence (RL) of SCFs was measured using a detector based on the hybrid based on hybrid PMT (DEP PPO 475B type) with maximum sensitivity in the 200-400 nm range and multi-channel registration system under excitation by $^{241}Am$ sources (5.5 MeV α-particles) in comparison with standard samples of YAP:Ce SC scintillators (Table 1).

## 3. Experimental results

**3.1. Light yield measurements.** We have found the strong competition between $Bi^{3+}$ and $Pr^{3+}$ ions in the energy transfer processes in LuAG:Pr,Bi and YAG:Pr,Bi SCF phosphors under high-energy excitation by e-beam or α-particles $Pu^{239}$ source (5.15 eV). This competition leads to strong decreasing the scintillation LY of LuAG:Pr and YAG:Pr SCF phosphors, grown from the $Bi_2O_3$ based fluxes, in comparison with the SCF analogues of these garnets, prepared from PbO-based fluxes (see Table 1). Lower LY of LuAG:Pr and YAG:Pr SCFs, grown by LPE from $Bi_2O_3$ flux even at relatively high (above 950°C) temperatures, is caused by the substantially large $Bi^{3+}$ content in these scintillators (in the range from several tens up to 1-2 at. %) in comparison with the typical $Pb^{2+}$ contamination (usually less than 0.01 at. %) in the mentioned SCF, grown from the PbO-based flux at relatively the same growth conditions (see Table 1). The reason for such significant differences in the concentration of flux-related impurities in the mentioned SCFs is higher segregation coefficient of $Bi^{3+}$ ions at LPE growth of YAG and LuAG SCFs from $Bi_2O_2$ flux, in comparison with that for $Pb^{2+}$ ions at LPE crystallization of these SCFs from PbO-based flux due to the significant differences in their ionic radii [26].

**3.2. Absorption spectra.** Absorption spectra of LuAG:Bi, YAG:Bi, LuAG:Bi,Pr and YAG:Bi,Pr SCFs in comparison with the absorption spectra of LuAG:Pr and YAG:Pr SCFs, grown from the traditional PbO flux, are shown in Fig.1 a and Fig.1 b.

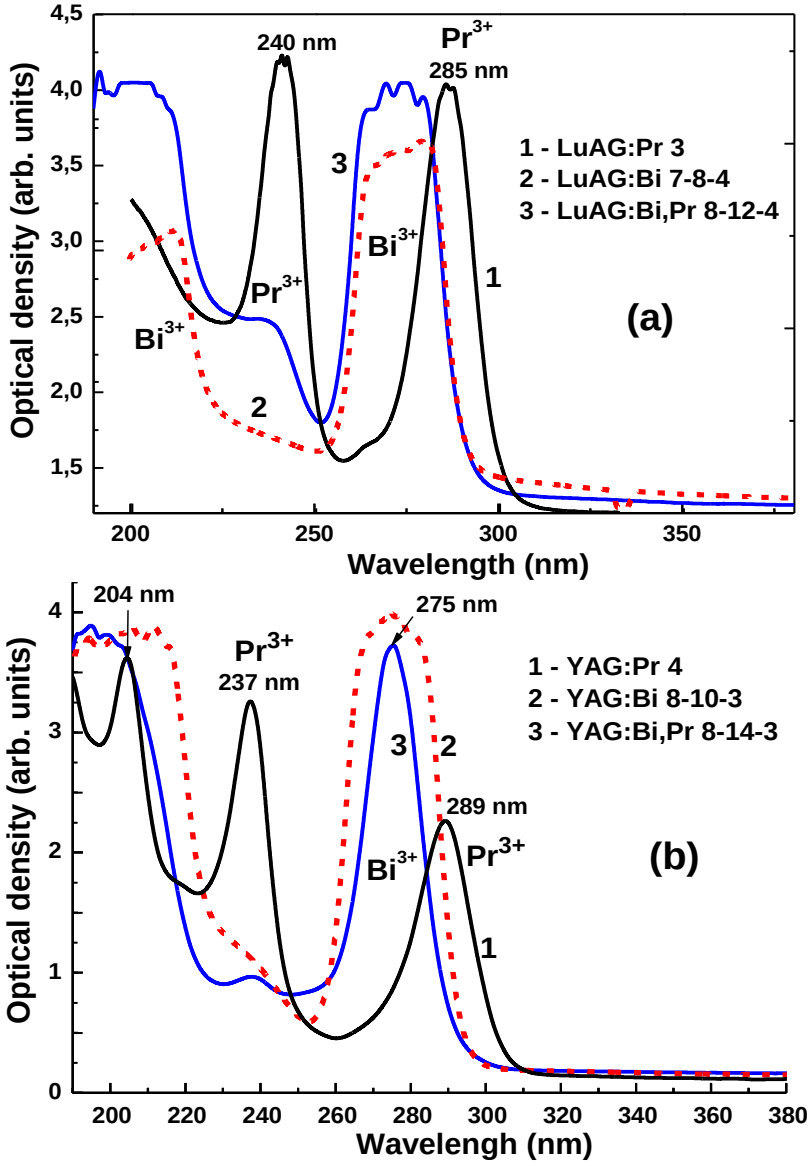


Fig.1. Absorption spectra in 190-400 nm range of LuAG:Pr (1a), LuAG:Bi (2a), LuAG:Bi,Pr (3a), YAG:Pr (1b), YAG:Bi (2b) and YAG:Bi,Pr (3b) SCF at 300 K

The absorption spectra of Bi and Bi-Pr doped LuAG and YAG SCF in 190-400 nm range consist of two strong absorption bands peaked at 270-275 nm and ~200 nm, related to the $^1S_0 \rightarrow {}^3P_1$ and $^1S_0 \rightarrow {}^1P_1$ transitions of $Bi^{3+}$ ions (A and C bands, respectively) [26]. Apart from these bands, the absorption spectra of Bi-Pr and Pr doped LuAG and YAG SCFs also contain the two bands, peaked at 240 and 285 nm (LuAG) and 237 and 289 nm (YAG), assigned to the 4f $(^3H_4) \rightarrow 5d_{1,2}$ transitions of $Pr^{3+}$ ions [8]. The difference in position of the absorption bands of $Pr^{3+}$ and $Bi^{3+}$ ions, related to the above mentioned transitions in LuAG and YAG hosts, is caused by the difference in the crystal field strength in the dodecahedral positions of garnet lattices, where large $Bi^{3+}$ and $Pr^{3+}$ ions (1.126 and 1.17 Å, respectively, in 8-fold coordination [34]) are localized.

The absorption spectra of Pr- and Bi-Pr doped SCF LuAG and YAG SCF in the visible (400-800 nm) range also contain the 4f–4f absorption bands of $Pr^{3+}$ ions around 500 nm ($^3P_{0,1,2} \rightarrow {}^3H_4$ transitions) and 600 nm ($^1D_2 \rightarrow {}^3H_4$ transitions) [8] (not shown in Fig.1).

**3.3. Cathodoluminescence (CL) spectra.** The CL spectra of LuAG:Bi, LuAG:Bi,Pr and YAG:Bi, YAG:Bi,Pr SCFs, grown from the $Bi_2O_3$ flux, in comparison with the CL spectra of LuAG:Pr

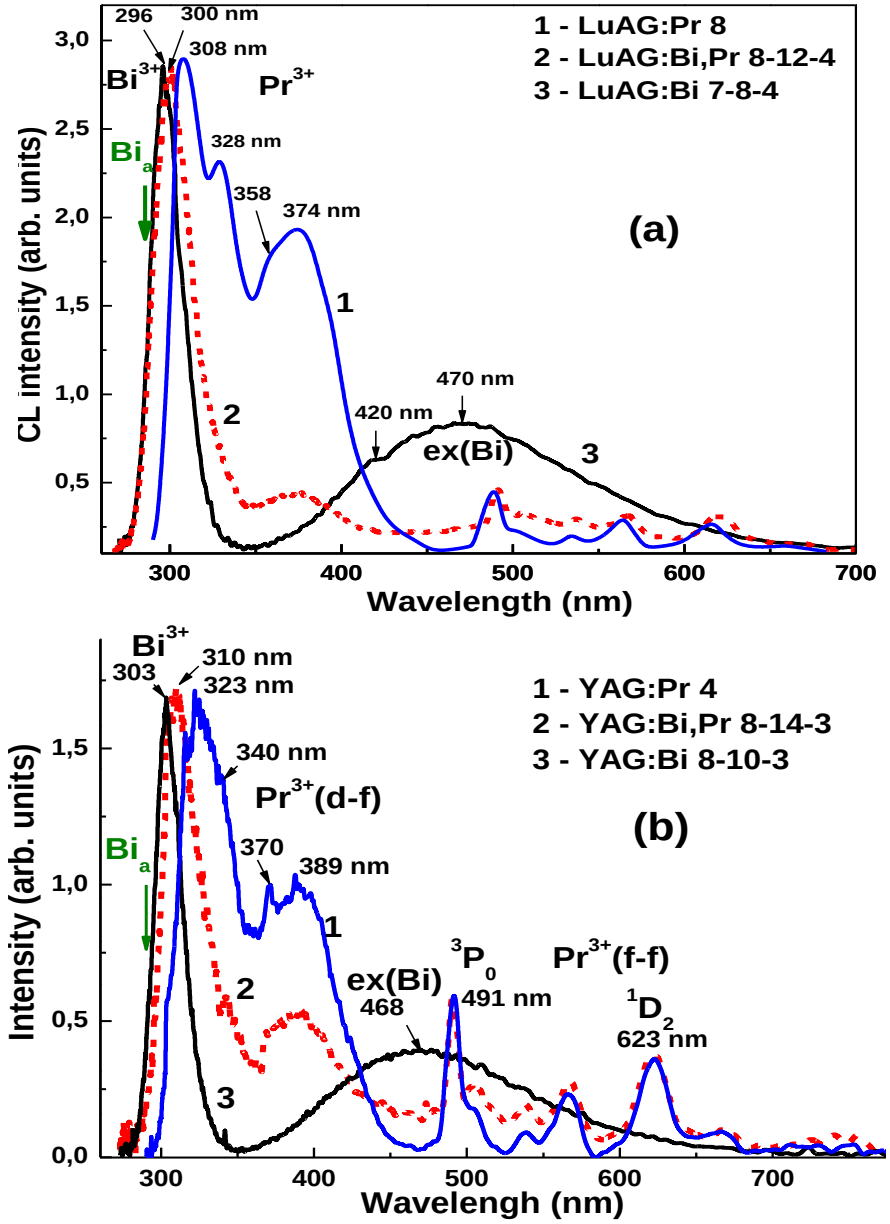


Fig.2. CL spectra of LuAG:Pr (1a), LuAG:Bi,Pr (2a) and LuAG:Bi (3a), YAG:Pr (1b), YAG:Bi,Pr (2b) and YAG:Bi (3b) SCFs at 300 K. The arrows indicate the maxima of $Bi^{3+}$ absorption bands (see Fig.1).

and YAG:Pr SCFs, grown from the PbO-based flux, are shown in Fig.2 a and Fig.2 b, respectively. The CL spectra of LuAG:Pr and LuAG:Bi,Pr SCF as well as YAG:Pr and YAG:Bi,Pr SCFs at 300 K (Fig.1, curves 1 and 2, respectively) show the $Pr^{3+}$ luminescence in the UV (280-450 nm) range in the four main bands peaked at 308, 328, 358 and 374 nm (LuAG) and 328, 340, 370 and 389 nm (YAG) caused by the allowed $5d^14f^1 \rightarrow 4f^2$ ($^3H_4$, $^3H_5$, $^3H_6$, $^3F_{3(4)}$) transitions of $Pr^{3+}$ ions [8]. The different positions of these bands of YAG and LuAG hosts are well correlated with the respective changes in the position of the $Pr^{3+}$ absorption bands in these garnets (Fig.1a and 1b, respectively, curves 1). Specifically, the high-energy shift of the emission spectrum and decrease of the energy distance between the emission bands of $Pr^{3+}$ ions occur for LuAG:Bi,Pr SCF in comparison with the position of these bands in YAG:Bi,Pr SCF which are caused by the smaller crystal field strength in the dodecahedral positions of LuAG lattice in comparison with YAG lattice.

The CL spectra of LuAG:Bi, YAG:Bi, LuAG:Bi,Pr and YAG:Bi,Pr SCFs show the intensive UV luminescence in the bands peaked at 296 and 303 nm, respectively, related to the $^3P_1 \rightarrow {}^1S_0$ transitions of $Bi^{3+}$ ions [24-29] (Fig.2a and 2b, curves 2 and 3, respectively). In the visible range the CL spectra of YAG:Bi and LuAG:Bi SCFs (Fig.2a and 2b, curves 3) also consists of the complex emission bands caused by superposition of the luminescence of excitons localized at $Bi^{3+}$ *single* and *dimer* centers in the bands peaked approximately at 470 and 420 nm (LuAG) at 468 and 423 nm (YAG), respectively [24-29].

From Figs.2a and 2b, we have noted that:

- intensity of the $Pr^{3+}$ luminescence in LuAG:Bi,Pr and YAG:Bi,Pr SCFs is significantly lower than that in the LuAG:Pr and YAG:Pr counterparts (Figs.2a and 2b, curves 2 and 1, respectively). This can reflect the strong competition of $Bi^{3+}$ and $Pr^{3+}$ ions in the energy transfer processes. Practically the CL spectra of LuAG:Bi,Pr and YAG:Bi,Pr SCFs present superposition of the $Pr^{3+}$ and $Bi^{3+}$ luminescence with the dominant contribution of the emissions of $Bi^{3+}$ ions due to significantly larger Bi concentration in these film in comparison with the content of Pr ions (Table 1);

- both UV emission bands related to the intrinsic luminescence of $Bi^{3+}$ ions in LuAG:Bi,Pr and YAG:Bi,Pr SCFs (Figs.2a and 2b, curves 2) are overlapped with the $4f^2 \rightarrow 5d^14f^1$ absorption bands of $Pr^{3+}$ ions peaked at 285 and 289 nm, respectively (Figs.1a and 1b, curves 1). Such re-absorption of the UV emission of $Bi^{3+}$ ions by the absorption bands of $Pr^{3+}$ ions leads to the $Bi^{3+} \rightarrow Pr^{3+}$ energy transfer resulted in the $Pr^{3+}$ luminescence in the UV range;

- both VIS emission bands related to the exciton emission in YAG:Bi,Pr and LuAG:Bi,Pr SCF (Figs.2a and 2b, curves 2) are strongly overlapped with the 4f-4f absorption bands of $Pr^{3+}$ ions in the visible range (not shown in Figs.1a and 1b due to very low thickness of the films). Such re-absorption of the emission of exciton localized at $Bi^{3+}$ centers by the f-f absorption bands of $Pr^{3+}$ ions leads to another kinds of the $Bi^{3+} \rightarrow Pr^{3+}$ energy transfer resulted in the slow f-f $Pr^{3+}$ luminescence in the VIS range.

**3.4. Excitation spectra.** The excitation spectra of the d-f and f-f $Pr^{3+}$ luminescence at 300 K in LuAG:Bi,Pr and YAG:Bi,Pr SCFs, monitored at 330 and 609 nm, are shown in Figs. 3a and 3b (curves 1 and 2, respectively), in comparison with the excitation spectra of the d-f $Pr^{3+}$ luminescence in LuAG:Pr and YAG:Pr SCFs, monitored at 320 nm (Fig.3a and 3b, curves 3). The excitation bands of the $Pr^{3+}$ luminescence in LuAG:Bi,Pr and YAG:Bi,Pr SCFs, peaked at 5.13 and 5.20 eV, respectively, coincide with the absorption band of $Pr^{3+}$ ions (Figs.1a and 1b, curves 1) and excitation bands of $Pr^{3+}$ luminescence (Figs.3a and 3b, curves 3) in the LuAG:Pr and YAG:Pr SCFs, respectively. At the same time, the low-energy excitation bands of the $Pr^{3+}$ luminescence, peaked at 4.40 and 4.39 eV in the spectra of LuAG:Pr and YAG:Pr SCFs (Figs.3, curves 3), practically are not observed in the spectra of LuAG:Bi,Pr and YAG:Bi,Pr SCFs (Figs.3a and 3b, curves 2 and 3) due to the complete overlapping with the A-excitation bands of the intrinsic $Bi^{3+}$ luminescence, related to the $^1S_0 \rightarrow {}^3P_1$ transitions of $Bi^{3+}$ ions.

Apart from the above mentioned bands, the excitation spectra of the $Pr^{3+}$ luminescence in LuAG:Bi,Pr and YAG:Bi,Pr SCFs contain also several other bands, related to the excitation of $Bi^{3+}$ luminescence. Namely, the A-bands peaked at 4.26-4.80 eV and 4.27-4.58 eV as well as the C-bands

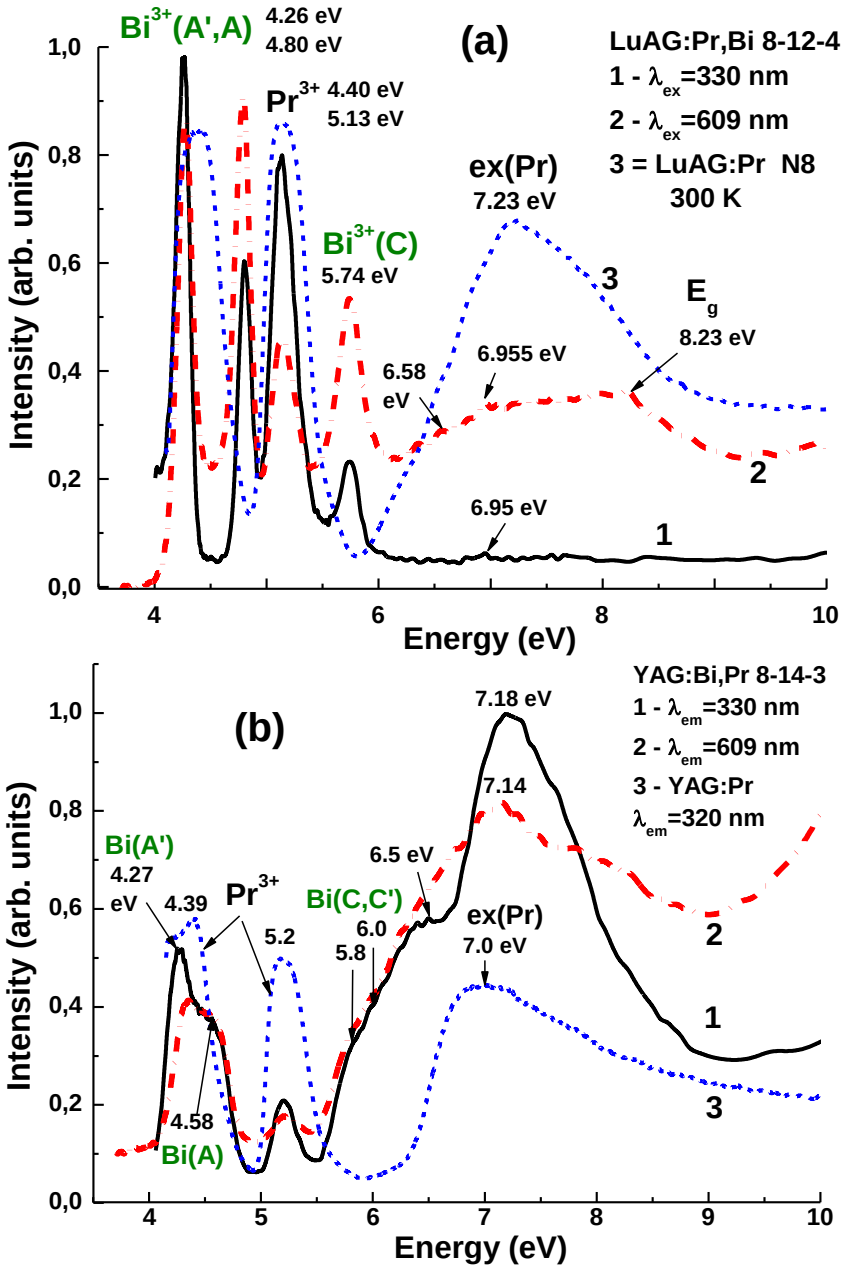


Fig.3. Excitation spectra of d-f (1) and f-f (2) luminescence of $Pr^{3+}$ ions in LuAG:Bi,Pr (a) and YAG:Bi,Pr (b) SCFs (a), monitored at a wavelength of 330 nm (curves 1) and 609 nm (curves 2), respectively, in comparison with the excitation spectra of d-f luminescence in LuAG:Pr SCF (a) and YAG:Pr (b) SCF, monitored at a wavelength of 310 nm (curves 3). T=300 K

peaked at 5.8 eV and 5.74 correspond to the intrinsic $^1S_0 \rightarrow {}^3P_1$ and $^1S_0 \rightarrow {}^1P_1$ transitions in $Bi^{3+}$ centers in LuAG and YAG hosts, respectively [see [25] for details]. It is necessary to note here that position of the A bands in LuAG:Bi,Pr and YAG:Bi,Pr SCF can not be determined with good accuracy due to the very large absorption of these SCFs in the 255-290 nm range (optical density is equal to 2-4, see Fig.1). As a result, the strong A-bands in the excitation spectra of these SCFs are separated in two A,A' sub-bands, peaked 4.26 and 4.80 eV (LuAG) and 4.27 and 4.58 eV (YAG).

The bands peaked at 6.58 eV in the excitation spectra of LuAG:Bi,Pr SCF and at 6.5 eV in the spectra of YAG:Bi,Pr SCF can be assigned to the charge transfer transition (CTT) between the oxygen ligands and $Bi^{3+}$ ions ($O^{2-} \rightarrow Bi^{3+}$ CTT). The excitation bands peaked at 7.0 and 7.23 eV as well as at 6.995 eV and 7.14-7.8 eV in the range of fundamental absorption edge of LuAG and YAG hosts can correspond to formation of excitons bound with the $Bi^{3+}$ and $Pr^{3+}$ ions, respectively. Peaks around 8.2 eV and 8.0 are related to onset of interband transitions in LuAG and YAG hosts, respetively [16, 17].

Presence of the $Bi^{3+}$ related bands in the excitation spectrum of the $Pr^{3+}$ luminescence confirms the existence of the efficient $Bi^{3+} \rightarrow Pr^{3+}$ energy transfer in LuAG:Bi,Pr and YAG:Bi,Pr SCFs. It is important to note that shape of the excitation spectra of the d-f and f-f $Pr^{3+}$ luminescence is very close to excitation spectra of the VIS emission of $Bi^{3+}$ based centers in YAG:Bi and LuAG:Bi SCFs; e.g., the energy from $Bi^{3+}$ to $Pr^{3+}$ ions is transferred both via re-absorption of the $Bi^{3+}$ UV emission by the $Pr^{3+}$ absorption bands in the UV range and by re-absorption of the VIS luminescence of excitons localized around Bi ions by the f-f absorption bands of $Pr^{3+}$ ions in the visible range (not shown in Fig.1). Excitation of the f-f luminescence corresponding to the radiative transition from $^1D_2$ level in LuAG:Bi,Pr and YAG:Bi,Pr SCF can also occur via the d-f luminescence of $Pr^{3+}$ ions (cooperative processes). The last mechanism has been described by some of us in detail in our previous paper [11].

**3.5. Decay kinetics of $Pr^{3+}$ and $Bi^{3+}$ luminescence.** The presence of effective energy transfer between the $Bi^{3+}$ ions and $Pr^{3+}$ ions in LuAG and YAG hosts is strongly supported by the decay kinetics of the $Pr^{3+}$ and $Bi^{3+}$ luminescence in LuAG:Bi,Pr and YAG:Bi,Pr SCFs (Figs.4 and 5). These figures present the decay kinetics of the d-f $Pr^{3+}$ emission at 300 K in LuAG:Pr and YAG:Pr SCFs and LuAG:Bi,Pr and YAG:Bi,Pr SCFs under excitation in the $4f^15d^1$-$5d^2$ absorption band of $Pr^{3+}$ ions at 240 nm in comparison with decay kinetics of the $Pr^{3+}$ luminescence (Fig.4) and $Bi^{3+}$ luminescence (Fig.5) in LuAG:Bi,Pr and YAG:Bi,Pr SCFs in under excitation in A-absorption band of $Bi^{3+}$ ions at 260 nm.

The decay kinetics of the d-f $Pr^{3+}$ luminescence in the mentioned LuAG:Pr and YAG:Pr SCFs under excitation in the 4f-5d absorption bands of $Pr^{3+}$ ions at 340 nm is close to exponential course with a decay time of the main components of 17 and 13 ns, respectively (Figs. 4a and 4b, curves 1). The second low-intensity component in the decay of the $Pr^{3+}$ luminescence with decay time in 120-130 ns range arises from the $Pb^{2+}$ flux related dopant presence in these SCFs and their influence on the decay kinetics of the $Pr^{3+}$ luminescence [6, 7]. The decay kinetics of the d-f $Pr^{3+}$ luminescence in LuAG:Bi,Pr and YAG:Bi,Pr SCFs under the same conditions of excitation is also close to exponential with the decay time of main components of 19 and 13 ns, respectively (Fig.4a and 4b, curves 2). The second low-intensity component of the $Pr^{3+}$ emission with decay time in the 230-310 ns range arises mainly from overlap of the $Pr^{3+}$ and $Bi^{+}$ luminescence in the UV range (Figs.2a and 2b).

The decay kinetics of the $Pr^{3+}$ luminescence in LuAG:Bi,Pr and YAG:Bi,Pr SCFs becomes slower under excitation in the A-absorption bands of $Bi^{3+}$ ions (Figs. 3a and 3b, curves 3). Apart from the fast components with a decay time of 33 and 43 ns, related to the radiative intrinsic $5d^2$-$5d^14f^1$ transition of $Pr^{3+}$ ions, the decay kinetics of the $Pr^{3+}$ luminescence in LuAG:Bi,Pr and YAG:Bi,Pr SCFs also contains two slow decay components with decay time in the hundred ns range (110-200 ns and 950-1300 ns), related to the energy transfer to $Pr^{3+}$ ions via the luminescence of $Bi^{3+}$ ions. This conclusion is confirmed by decay kinetics of the intrinsic $Bi^{3+}$ luminescence in the UV range, presented in Fig.5a and 5b, curves

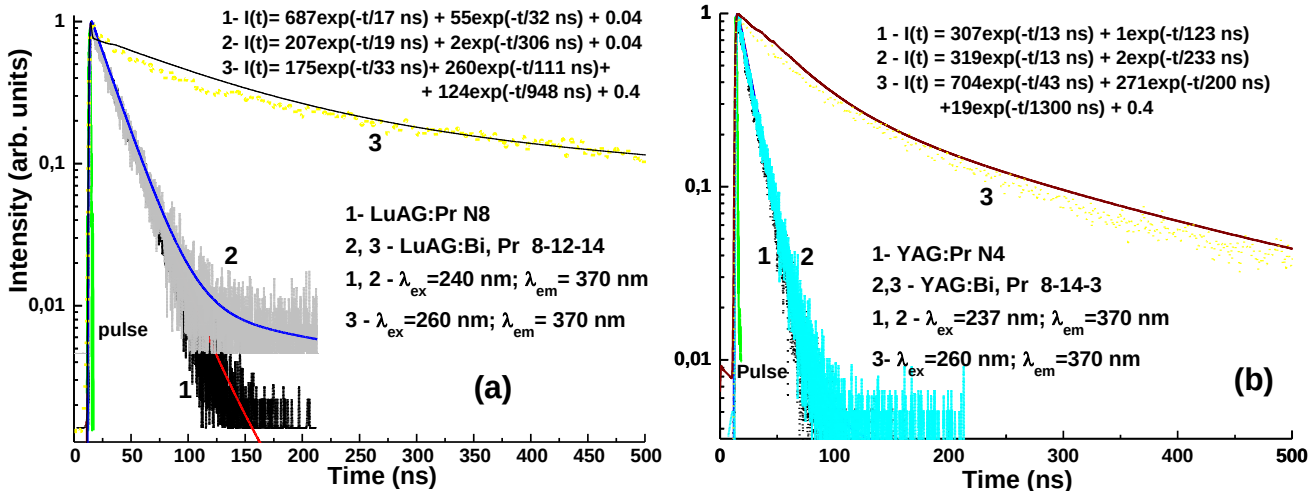


Fig.4. Decay kinetics of luminescence of $Pr^{3+}$ ions at 370 nm in LuAG:Pr (1a), LuAG:Bi,Pr (2a, 3a), YAG:Pr (1b) and YAG:Bi,Pr (2b, 3b) SCFs under excitation in the absorption bands of $Pr^{3+}$ ions at 240 nm (1, 2) and $Bi^{3+}$ ions at 260 nm (3). The approximations of decay curves are given by the solid lines.

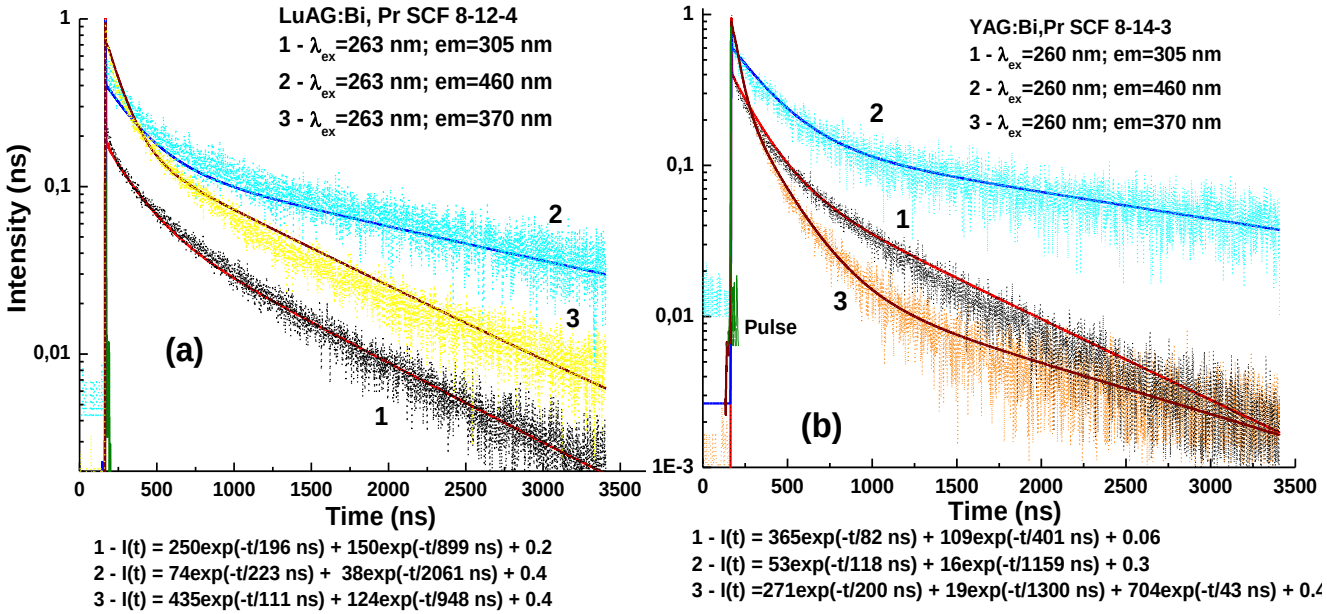


Fig.5. Decay of $Bi^{3+}$ luminescence at 305 nm (curves 1) and 460 nm (curves 2) and $Pr^{3+}$ luminescence at 370 nm (3), respectively in LuAG:Bi,Pr (a) and YAG:Bi,Pr (b) SCF under excitation in absorption band of $Bi^{3+}$ ions at 260 nm.

1, where the two components of emission with decay times of 80-200 ns and 400-800 ns, respectively, were noted. In comparison with the main components of decay kinetics of $Bi^{3+}$ ions in LuAG:Bi and YAG:Bi SCFs (120-330 ns and 1250-2300 ns, respectively [22]), the lifetimes of the intrinsic $Bi^{3+}$ luminescence in LuAG:Bi,Pr and YAG:Bi,Pr SCFs is notably smaller.

Due to the overlap of the VIS band of excitons localized around $Bi^{3+}$ centers with the absorption bands of $Pr^{3+}$ ions, another kind of $Bi^{3+}\rightarrow Pr^{3+}$ energy transfer is observed in LuAG:Bi,Pr and YAG:Bi,Pr SCFs, resulted in the appearance of the slow f-f luminescence of $Pr^{3+}$ ions in the visible range. This conclusion is confirmed by decay kinetics of the visible luminescence of excitons around Bi ions in these SCFs, presented in Fig.5 a and 5b, curves 2, where two components of the emission with decay times of 120-220 ns and 1060-2060 ns, respectively, were found. In comparison with the decay time of the main components of the same exciton emission in LuAG:Bi and YAG:Bi SCFs (170-385 ns and 1850-2450 ns, respectively [22]), the lifetime of the intrinsic $Bi^{3+}$ luminescence in LuAG:Bi,Pr and YAG:Bi,Pr SCFs was also notably smaller.

**Conclusions**

The room-temperature absorption, cathodoluminescence, excitation spectra of photoluminescence and decay kinetics of photoluminescence were studied for $Bi^{3+}$ and $Bi^{3+}$-$Pr^{3+}$doped $Lu_3Al_5O_{12}$ (LuAG) and $Y_3Al_5O_{12}$ (YAG) single crystalline films (SCF) grown by the liquid phase epitaxy method from the $Bi_2O_3$-based flux. Apart from the $Pr^{3+}$ related emission bands in the UV (280-400 nm range), the luminescence bands in the UV range at 296 and 303 nm arising from the intrinsic radiative transitions of $Bi^{3+}$-centers, and emission bands in the visible range at 486 and 470 nm, related to the luminescence of excitons localized around Bi-based centers, were identified in both Bi-doped LuAG and YAG SCFs.

We have evidenced the competition between $Bi^{3+}$ and $Pr^{3+}$ ions in the energy transfer processes from the LuAG and YAG hosts to these ions under band-to-band excitation. This competition leads to strong decreasing the scintillation light yield of LuAG:Pr and YAG:Pr SCF phosphors, grown from the $Bi_2O_3$ based fluxes, in comparison with the SCF analogues of these garnets, prepared from PbO-based fluxes. The reason for such a LY decrease is the higher segregation of $Bi^{3+}$ ions in comparison with the segregation of $Pb^{2+}$ ions at crystallization of garnet SCFs from mentioned fluxes due to the significant differences in their ionic radii (1.17 and 1.29 Å, respectively). As a result of such differences, the substantially large $Bi^{3+}$ content (even in the range from several tens to 1-2 at. %, see Table 1) can be

realized in LuAG:Pr and YAG:Pr SCF phosphors grown by LPE onto YAG substrates from $Bi_2O_3$ flux at relatively high (above 950$^oC$) temperatures, in comparison with the typical $Pb^{2+}$ contamination in the mentioned SCFs, grown from the PbO-based flux at the same growth conditions (usually less than 0.01 at. %).

The energy transfer processes from the host lattice to $Bi^{3+}$ and $Pr^{3+}$ ions and from $Bi^{3+}$ to $Pr^{3+}$ ions were investigated $Bi^{3+}$-$Pr^{3+}$ doped LuAG and YAG SCFs under excitation by synchrotron radiation with energy in the 3.7-10 eV range. Due to overlap of the UV emission band of $Bi^{3+}$ centers with the absorption band of $Pr^{3+}$ centers peaked at 285-290 nm, an effective radiative energy transfer from $Bi^{3+}$ ions to $Pr^{3+}$ ions takes place in the mentioned films, resulting in the appearance of slower component in the hundred ns range in the luminescence decay kinetics of the d-f emission of $Pr^{3+}$ ions. The overlap of the emission band of excitons localized around $Bi^{3+}$ centers with the absorption band of $Pr^{3+}$ ions in the visible range, leads also to another kind of $Bi^{3+}\rightarrow Pr^{3+}$ energy transfer in the mentioned films, resulting in appearance of the slow f-f luminescence of $Pr^{3+}$ ions in the visible range. Other reason for Bi-Pr energy transfer in our Bi-Pr doped YAG and LuAG SCF samples is the dipole-dipole interaction between the $Bi^{3+}$ and $Pr^{3+}$ ions. The role of such a mechanism of energy transfer strongly increases with the increasing the concentration of both dopants. We plan to investigate such type transfer in LuAG:Bi,Pr and YAG:Bi,Pr SCF phosphors in more detail in our future paper.

## Acknowledgements

The work was supported by Ukrainian Ministry of Education and Science (project SF-126F), Czech Science Foundation project No 202/08/0893 and NATO CBP.NUKR.CLG984305 projects. The measurements at the Superlumi station were performed in the framework of HASYLAB I-20110085 EC and I-20110938 EC research projects. The authors express their gratitude to dr. W. Drube and dr. A. Kotlov from HASYLAB, DESY for their assistance in carrying out the experiments in HASYLAB at DESY.

## References

1. A. Wojtowicz, W. Drozdowski, D. Wisniewski, J. Lefaucheur, Z. Galazka, Zh. Gou, T. Lukasiewicz, J. Kisielewski, Optical Materials**,** 28 (2006) 85.
2. H. Ogino, A. Yoshikawa, M. Nikl, A. Krasnikov, K. Kamada, T. Fukuda, J. Cryst. Growth, 287 (2006) 335.
3. T. Yanagida, M. Sato, K. Kamada, A. Yoshikawa, F. Saito, IEEE Nuclear Science Symposium Conference Record, 2 (2007) 1338.
4. K. Kamada, R.T. Yanagida, J. Kataoka, A. Yoshikawa, A. Fukabori, K. Tsutsumi, T. Endo, Y. Usuki, IEEE Nuclear Science Symposium Conference Record (NSS/MIC), (2009) 1949.
5. L. Swiderski, M. Moszynski, A. Nassalski, A. Syntfeld-Kazuch, T. Szczesniak, K. Kamada, K. Tsutsumi, Y. Usuki, T. Yanagida, A. Yoshikawa, W. Chewpraditkul, M. Pomorski, IEEE Nuclear Science Symposium Conference Record, 56 (2008) 2840.
6. J. Pejchal, M. Nikl, E. Mihóková, J.A. Mareš, A. Yoshikawa, H. Ogino, K.M. Schillemat, A. Krasnikov, A. Vedda, K. Nejezchleb, V. Múčka, J. Phys. D: Appl. Phys., 42 (2009) 055117.
7. Y. Nakagawa, J. Kawarabayashi, K. Watanabe, H. Tomita, H. Toyokawa, K. Kamada, T. Yanagida, A. Yoshikawa, T. Iguchi, Progress in Nuclear Science and Technology, 1 (2011) 285.
8. T. Yanagida, M. Sato, K. Kamada, Y. Fujimoto, Y. Yokota, A. Yoshikawa, V. Chani, Optical Materials, 33 (2011) 413.
9. Yu. Zorenko, V. Gorbenko, M. Nikl, J. A. Mares, T. Martin, P.-A. Douissard, IEEE Trans. Nucl. Sci., 57 (2010) 1335.
10. Yu. Zorenko, V. Gorbenko, V. Savchyn, T. Voznyak, M. Nikl, J.A. Mares and A. Winnacker, Radiation measurements, 45 (2010) 441.
11. V. Gorbenko, Yu. Zorenko, V. Savchyn, T. Zorenko, A. Pedan, V. Shkliarskyi, Radiation Measurements, 45 (2010) 461.
12. V. Gorbenko, A. Krasnikov, M. Nikl, S. Zazubovich, Yu. Zorenko, Optical Materials, 31 (2009) 1805.

13. A. Koch, C. Raven, P. Spanne, A. Snigirev, J. Opt. Soc. Am., A 15 (1998) 1940.
14. A. Koch, F. Peyrin, P. Heurtier, B. Chambaz, B. Ferrand, W. Ludwig, M. Couchaud, Proc SPIE, 3659 (1999) 170.
15. T. Martin, A. Koch, Journal of Synchrotron Radiation, 13 (2006) 180.
16. T. Martin, P.-A. Douissard, M. Couchaud, A. Cecilia, T. Baumbach, K. Dupre, A. Rack, IEEE Transactions on Nuclear Science, 56 (2009) 1412.
17. Yu. V. Zorenko, L. N. Limarenko, I. V. Nazar and M. V. Pashkovskii, Journal of Applied Spectroscopy, 55 (1991) 1100.
18. Yu. Zorenko, A. Voloshinovskii, I. Konstankevych, V. Kolobanov, V. Mikhailin, D. Spassky. Radiation Measurements, 38 (2004) 677.
19. Yu. Zorenko, A. Voloshinovskii, V. Savchyn, T. Vozniak, M. Nikl, K. Nejezchleb, V. Mikhailin, V. Kolobanov, D. Spassky, Phys. Stat. Sol. (b), 244 (2007) 2180.
20. Yu. Zorenko, V. Gorbenko, E. Mihokova, M. Nikl, K. Nejezchleb, A. Vedda, V. Kolobanov, D. Spassky, Radiation Measurements, 42 (2007) 521.
21. M. Nikl, J. Pejchal, E. Mihokova, J. A. Mares, H. Ogino, A. Yoshikawa, T. Fukuda, A. Vedda, C. D'Ambrosio, Appl.Phys. Letters, 88 (2006) 141916.
22. M. Nikl, E. Mihokova, J. Pejchal, A. Vedda, M. Fasoli, I. Fontana, V. Laguta, V.V. Babin, K. Nejezchleb, A. Yoshikawa, H. Ogino, G. Ren, IEEE Trans. Nucl. Sci., 55 (2008) 1035.
23. G.B. Scott, J.L. Page, J. Appl. Phys., 48 (1977) 1342.
24. V. Babin, V. Gorbenko, A. Makhov, J.A. Mares, M. Nikl, S. Zazubovich, Yu. Zorenko, Journal of Luminescence, 127 (2007) 384.
25. Yu. Zorenko, V. Gorbenko, T. Voznyak, V. Vistovsky, S. Nedilko, M. Nikl, Radiation Measurements, 42 (2007) 882.
26. Yu. Zorenko, J. A. Mares, R. Kucerkova, V. Gorbenko, V. Savchyn, T. Voznyak, M. Nikl, A. Beitlerova, K. Jurek, J. Phys. D: Appl. Phys., 42 (2009) 075501.
27. V. Babin, V. Gorbenko, A. Krasnikov, A. Makhov, M. Nikl, K. Polak, S. Zazubovich, Yu. Zorenko, J. Phys.: Condens. Matter., 21 (2009) 415502.
28. V. Babin, V. Gorbenko, A. Krasnikov, A. Makhov, M. Nikl, S. Zazubovich, Yu. Zorenko Radiation Measurements, 45 (2010) 331.
29. Yu. Zorenko, V. Gorbenko, T. Voznyak, V. Jary, M. Nikl, Journal of Luminescence, 130 (2010) 1963.
30. D.E. Lacklinson, G.B. Scott, G.L. Page, Solid State Commun., 14 (1974) 861.
31. Ja. M. Zakharko, V. A. Andrijchyk, Journal Applied Spectroscopy, 38 (1983) 381.
32. M. Ilmer, B.C. Grabmaier, G. Blasse, Chem. Mater., 6 (1994) 204.
33. A.A. Setlur, A.M. Srivastava, Optical Materials, 29 (2006) 410.
34. http://abulafia.mt.ic.ac.uk/ shannon/ radius.php.